

## OSCILLATIONS IN ATMOSPHERES WITH TOPS

R. S. LINDZEN\*

National Center for Atmospheric Research, Boulder, Colo.

E. S. BATTEN

The RAND Corporation, Santa Monica, Calif.

J.-W. KIM

University of California, Los Angeles, Calif.

### ABSTRACT

Free and forced oscillations are compared for infinite and bounded atmospheres. Both continuous and two layer bounded atmospheres are considered. It is found that bounded atmospheres reproduce the free oscillations of the infinite atmosphere with accuracy that depends on top height—they, however, also introduce spurious free oscillations. In studying forced oscillations, the spurious oscillations of bounded atmospheres appear as spurious resonances. In general, bounded atmospheres do not properly respond to oscillations that propagate vertically.

### 1. INTRODUCTION

It is common practice to use simplified calculations in order to elucidate the nature of various more complicated atmospheric problems. As pointed out by Lindzen [3], a variety of such problems is included in the consideration of linearized perturbations on a static basic state (or one with a "constant" zonal flow). Such a study gives a remarkably good description of Rossby-Haurwitz waves, atmospheric tides, and other features. It is clear that various multilevel numerical models do not correspond precisely to the real atmosphere—especially as concerns vertical resolution and the upper boundary. If the above mentioned simplified calculations had been carried out for prototypes of the model atmospheres rather than of the real atmosphere, what would have resulted? In this paper we will consider the behavior of free and thermally forced linear perturbations on a static isothermal atmosphere for three different models:

1. An infinite atmosphere where disturbances are required to remain bounded as  $z$  (i.e., altitude)  $\rightarrow \infty$ . If the disturbances propagate vertically, a radiation condition is imposed at great altitudes.

2. A bounded atmosphere where  $dp/dt=0$  at some upper boundary height.

3. A bounded atmosphere wherein the continuous vertical variation is approximated by a two layer model.

It will be shown that, under certain conditions, various classes of motions behave similarly in each of the models. However, there are always very significant differences as well. In particular, while models 2 and 3 can approximately reproduce the Rossby waves described by model

1, they also produce spurious Rossby waves. Also, models 2 and 3 can badly misrepresent thermal tides. Model 2 has been included primarily because it is toward this model that multilevel models converge as the number of levels is increased.

### 2. EQUATIONS

We consider the problem of linearized oscillations in a rotating, isothermal, spherical gaseous envelope. For purposes of considering forced responses we will include a thermal excitation of the form

$$J = J(\theta, \varphi, t)e^{-z/3}, \quad (1)$$

where  $\theta$ =colatitude,  $\varphi$ =longitude,  $t$ =time,  $x=z/H$ ,  $H = RT_0/g$ ,  $R$ =gas constant,  $g$ =acceleration of gravity,  $T_0$ =basic temperature, and  $J$ =heating per unit time per unit mass. The particular vertical structure chosen for  $J$  is of no particular significance. It happens to be the structure for excitation by insolation absorption by water vapor (Siebert [5]). The oscillations that exist when  $J=0$  are free oscillations; Rossby-Haurwitz waves are of this type.

It proves convenient to reduce the various equations for small oscillatory fields to a single equation for the following variable:

$$y = -\frac{e^{z/2}}{\gamma p_s} \omega \quad (2)$$

where  $\gamma = c_p/c_v = 1.4$ ,  $p_s$ =basic surface pressure,  $\omega = dp/dt$ , and  $p$ =pressure. The equation for  $y$  is separable in its  $\theta$ ,  $\varphi$ ,  $t$ , and  $z$  (or  $x$ ) dependence.<sup>1</sup>  $y$  may be written

\*Now at the University of Chicago.

<sup>1</sup> See Siebert [5], for example, for a complete development of these equations.

$$y = L(x)\Theta(\theta)e^{is\varphi}e^{i\sigma t}. \quad (3)$$

It is assumed that  $J$  will have the same  $t$  and  $\varphi$  dependence.  $\Theta(\theta)$  satisfies Laplace's Tidal Equation:

$$\frac{d}{d\mu} \left[ \frac{(1-\mu^2)}{f^2-\mu^2} \frac{d\Theta}{d\mu} \right] + \frac{1}{f^2-\mu^2} \left[ \frac{s}{f} \frac{f^2+\mu^2}{f^2-\mu^2} + \frac{s^2}{1-\mu^2} \right] \Theta + \lambda\Theta = 0, \quad (4)$$

where  $\mu = \cos \theta$ ,  $f = \frac{\sigma}{2\Omega}$ , and  $\Omega$  = earth's rotation rate.

$\lambda$  is the separation constant; it is usually written

$$\lambda = \frac{4a^2\Omega^2}{gh} \quad (5)$$

where  $a$  = earth's radius.  $h$ , known as the equivalent depth, replaces  $\lambda$ . The boundary conditions on  $\Theta$  are that it be bounded at the poles. When, for a given solution of (4),  $J$  can be expressed as

$$J = J(x)\Theta(\theta), \quad (6)$$

then  $L(x)$  satisfies

$$\frac{d^2 L}{dx^2} - \frac{1}{4} \left[ 1 - \frac{4\kappa H}{h} \right] L = \frac{\kappa J}{\gamma_s h} e^{-x/2} \quad (7)$$

where  $\kappa = 2/7$ .

The condition that  $w$  (vertical velocity) equal zero at  $x = 0$  implies

$$\frac{dL}{dx} + \left( \frac{H}{h} - \frac{1}{2} \right) L = 0, \quad (8)$$

at  $x = 0$ .

As  $x \rightarrow \infty$ , it is required that  $L$  remain bounded. If  $(4\kappa H/h - 1) > 0$ , this is an insufficient condition. It is usual to require, in addition, that there be no downcoming energy flux. These considerations are only relevant to an infinite atmosphere. In numerical models, it is usual to introduce the artifice of an atmosphere with a top at some height. At this height, it is usually required that

$$y = \omega = 0. \quad (9)$$

If one uses pressure instead of  $x$  (or  $z$ ) as a vertical coordinate (assuming motions are hydrostatic) then (7) becomes

$$\frac{d^2 \omega}{dp^2} + \frac{s}{h} \omega = -\frac{\kappa}{gh} \frac{1}{p} \left( \frac{p}{p_s} \right)^{1/3} J \quad (10)$$

where  $S = \kappa H/p^2$  (Nunn [4], Flattery [2]). The height perturbation is related to  $\omega$  as follows:

$$z' = \frac{h}{i\sigma} \frac{d\omega}{dp}. \quad (11)$$

The condition that  $w=0$  at  $x=0$  (i.e., at  $p=p_s$ ) becomes

$$\omega = g\rho \frac{\partial z}{\partial t} \text{ at } p=p_s, \quad (12)$$

where  $\rho$  = density;  $\rho_s = p_s/gH$ .

In studying free oscillations we solve (7) with  $J=0$ . In general there will be only a single  $h$  for which (7) has a nontrivial solution (Dikii [1]). However, when the atmosphere has an artificial top then there are an infinite number of  $h$ 's for which (7) has nontrivial solutions. For a bounded atmosphere approximated by  $N$  levels there will only be  $N$   $h$ 's since only  $N$  of the infinite number of vertical modes can be independently resolved. Given  $h$ , and specifying the zonal wave number,  $s$ , (4) with its boundary conditions constitutes an eigenfunction-eigenvalue problem where the eigenvalue is  $\sigma$  (or  $c$ , the phase speed, since  $s$  is known), and eigenfunctions for different  $c$ 's differ in their latitude wave number. These constitute the free oscillations of the atmosphere; they include Rossby-Haurwitz waves. In an infinite atmosphere these are all associated with a single  $h$ . Anticipating later results, it should be pointed out that bounded models will have other Rossby-Haurwitz waves associated with the spurious  $h$ 's.

For forced oscillations  $\sigma$  and  $s$  are specified. Equation (4), with its associated boundary conditions, then becomes an eigenvalue-eigenfunction problem where  $h$  is the eigenvalue.  $J$ 's latitude dependence is expanded in terms of the eigenfunctions (denoted by subscript  $n$ ) yielding

$$J = \sum_n J_n(x)\Theta_n(\theta)e^{i(\sigma t + s\varphi)}. \quad (13)$$

$y$  is similarly expanded, the vertical structure of each mode is obtained by solving (7) for each  $h_n$ . Each eigenfunction is associated with a different vertical structure; for each  $h_n$  we compute the atmosphere's response to  $J_n$ . If for some  $\sigma$  and  $s$  the resulting  $h_n$  is equal to that for free oscillations, then we will obtain an infinite response. Thus, an examination of forced responses for all values of  $h$  will also reveal the free oscillations.

### 3. RESPONSE FUNCTIONS

By considering (7) for all values of  $h$  we will, in effect, have computed the response of all forced oscillations—given the relation of  $h$  to  $\sigma$  and  $s$  [and some latitude wave number corresponding to the particular eigenfunction of (4)]. Similarly, where the response blows up yields the  $h$ 's for the free oscillations for which  $\sigma$  (or  $c$ ) is related to  $s$  and  $n$  (and some latitude wave number). In connection with the idea of "response" we have two problems: 1) what is it that we are studying the response to, and 2) what constitutes a response. Since we are primarily interested in the effects of lids and two layer approximations,

we will restrict ourselves to isothermal atmospheres and forcings of the form given in (1). As a measure of response we will use surface pressure. Let

$$J_n = \frac{i\sigma RT}{\kappa} \frac{\tau_n}{T} \Theta_n(\theta) e^{-x/3}, \quad (14)$$

where  $\tau_n$  = some measure of the temperature change that would occur in the absence of dynamics. Then the surface pressure response will be given by

$$\frac{\delta p_n}{p_s} = R(h_n) \frac{\tau_n}{T} \Theta_n(\theta), \quad (15)$$

where  $R$  is the nondimensional response function. Our problem is to evaluate  $R$ .<sup>2</sup>

For an infinite isothermal atmosphere the solution to (7) is

$$L = A e^{i\lambda x} + B e^{-i\lambda x} + \frac{i\sigma R}{\gamma g h} \frac{\tau}{(25/36 + \lambda^2)} e^{-5/6x} \quad (16)$$

if

$$\lambda^2 = \frac{1}{4} \left[ \frac{4\kappa H}{h} - 1 \right] > 0$$

and

$$L = A e^{\mu x} + B e^{-\mu x} + \frac{i\sigma R}{\gamma g h} \frac{\tau}{(25/36 - \mu^2)} e^{-5/6x} \quad (17)$$

if

$$\mu^2 = \frac{1}{4} \left[ 1 - \frac{4\kappa H}{h} \right] > 0.$$

In the first case [i.e., equation (16)], the radiation condition implies  $B=0$ . In the second case [i.e., equation (17)] boundedness requires that  $A=0$ . Applying (8), equations (16) and (17) become

$$L = \frac{i\sigma H \tau}{\gamma h T} \left\{ \frac{\frac{4}{3} \frac{H}{h}}{\left( \frac{25}{36} + \lambda^2 \right)} e^{i\lambda x} + e^{-5/6x} \right\}, \quad (18)$$

for

$$\lambda^2 = \frac{1}{4} \left[ \frac{4\kappa H}{h} - 1 \right] > 0,$$

and

$$L = \frac{i\sigma H \tau}{\gamma h T} \left\{ \frac{\frac{4}{3} \frac{H}{h}}{\left( \frac{25}{36} - \mu^2 \right)} e^{-\mu x} + e^{-5/6x} \right\}, \quad (19)$$

for

$$\mu^2 = \frac{1}{4} \left[ 1 - \frac{4\kappa H}{h} \right] > 0.$$

$\delta p/p_s$  at  $z=0$  is related to  $L$  as follows (Siebert [5]):

$$\frac{\delta p}{p_s} = \frac{i\gamma}{\sigma} L(0). \quad (20)$$

Hence,

$$R_1 = \frac{-\frac{H}{h}}{\left( \frac{25}{36} + \lambda^2 \right)} \left\{ \frac{\frac{5}{6} + i\lambda}{\frac{H}{h} - \frac{1}{2} + i\lambda} \right\} \quad (21)$$

for  $\lambda^2 > 0$   
and

$$R_1 = \frac{-\frac{H}{h}}{\left( \frac{25}{36} - \mu^2 \right)} \left\{ \frac{\frac{5}{6} - \mu}{\frac{H}{h} - \frac{1}{2} - \mu} \right\} \quad (22)$$

for  $\mu^2 > 0$ .

For a bounded, continuous atmosphere we take  $L=0$  at some top where  $x=x_t$ . Then we obtain

$$R_2 = \frac{-\frac{H}{h}}{\left( \frac{25}{36} + \lambda^2 \right)} \frac{\left[ \frac{5}{6} - \lambda \cot \lambda x_t + \frac{\lambda e^{-\frac{5x_t}{6}}}{\sin \lambda x_t} \right]}{\left[ \frac{H}{h} - \frac{1}{2} - \lambda \cot \lambda x_t \right]} \quad (23)$$

for  $\lambda^2 > 0$ ,  
and

$$R_2 = \frac{-\frac{H}{h}}{\left( \frac{25}{36} - \mu^2 \right)} \frac{\left[ \frac{5}{6} - \mu \coth \mu x_t + \frac{\mu e^{-\frac{5x_t}{6}}}{\sinh \mu x_t} \right]}{\left[ \frac{H}{h} - \frac{1}{2} - \mu \coth \mu x_t \right]} \quad (24)$$

for  $\mu^2 > 0$ .

In treating the two layer atmosphere we go over to pressure coordinates (see Thompson [6], for example). For the unperturbed state

$$\frac{z}{H} = -\log \left( \frac{p}{p_s} \right). \quad (25)$$

The condition that the perturbation vertical velocity be zero at the ground is given by equation (12), and the upper boundary condition is (9). In view of (14), equation (10) becomes

$$\frac{d^2 \omega}{dp^2} + \frac{S}{h} \omega = -\frac{i\sigma H}{p} \frac{\tau}{h T} \left( \frac{p}{p_s} \right)^{1/3}. \quad (26)$$

The levels are shown in figure 1.  $\omega$  is evaluated at levels 0, 1, 2.  $z'$  is evaluated at levels 1/2 and 3/2. Thus (26) becomes

$$\frac{\omega_2 - 2\omega_1 + \omega_0}{\delta p^2} + \frac{\kappa}{p_1^2} \frac{H}{h} \omega_1 = \frac{i\sigma H}{p_1} \frac{\tau}{h T} \left( \frac{p_1}{p_s} \right)^{1/3}, \quad (27)$$

<sup>2</sup>  $R$ , as used here, should be distinguished from  $R$  when used for the gas constant.

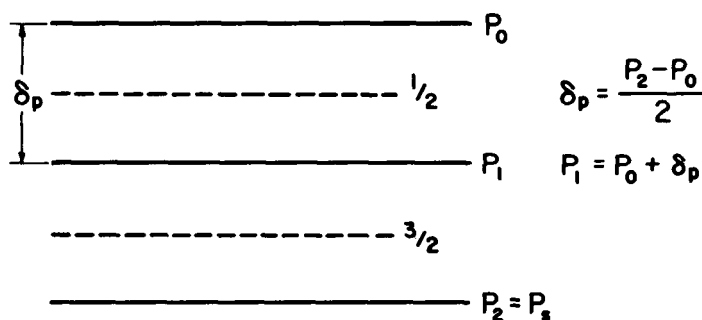


FIGURE 1.—Placement and labelling of levels for two layer calculations.

or

$$\frac{\omega_2 - 2\omega_1}{\delta p^2} + \frac{\kappa}{p_1^2} \frac{H}{h} \omega_1 = -\frac{i\sigma}{p_1} \frac{H}{h} \frac{\tau}{T} \left(\frac{p_1}{p_s}\right)^{1/3}, \quad (28)$$

since  $\omega_0$  has been taken as zero.<sup>3</sup> From (11) we have

$$z'_{1/2} = \frac{h}{i\sigma} \frac{\omega_1}{\delta p} \quad (29a)$$

and

$$z'_{3/2} = \frac{h}{i\sigma} \frac{\omega_2 - \omega_1}{\delta p}. \quad (29b)$$

In order to satisfy (12) we need  $z'$  at level 2. How one finds this in a model as crude as the two layer model is, at best, somewhat arbitrary; we have used linear extrapolation. Thus,

$$z'_2 = \frac{h}{i\sigma} \frac{1}{\delta p} \left( \frac{3}{2} \omega_2 - 2\omega_1 \right). \quad (30)$$

The important physical feature of (30) is that it shows that  $z'_2$  is a function of both  $\omega_2$  and  $\omega_1$ ; this particular feature does not depend on the use of linear extrapolation. Combining (28) and (30) we get

$$\omega_2 \left( 1 - \frac{1}{2} \left( \frac{H}{h} \frac{\delta p}{p_s} - \frac{3}{2} \right) \left( \frac{\kappa H}{h} \frac{\delta p}{p_1^2} - 2 \right) \right) = -\frac{i\sigma}{p_1} \frac{H}{h} \frac{\tau}{T} \left( \frac{p_1}{p_s} \right)^{1/3} \delta p^2. \quad (31)$$

Now  $\delta p$  at the ground equals  $i\sigma\omega_2$ , and therefore

$$R_3 = \frac{-\frac{H}{h} \left( \frac{p_1}{p_s} \right)^{1/3} \frac{\delta p^2}{p_1 p_3}}{\left( 1 - \frac{1}{2} \left( \frac{H}{h} \frac{\delta p}{p_s} - \frac{3}{2} \right) \left( \frac{\kappa H}{h} \frac{\delta p^2}{p_1^2} - 2 \right) \right)}. \quad (32)$$

Before proceeding to detailed discussion of  $R_1$ ,  $R_2$ , and  $R_3$ , several obvious differences in these response functions may be noted. First,  $R_2$  and  $R_3$  must be real;  $R_1$  need not be. This is merely a result of the fact that energy can escape upwards in an unbounded atmosphere while it cannot in a bounded atmosphere. With an energy-absorb-

ing lower boundary layer in the bounded models,  $R_2$  and  $R_3$  will become complex. Needless to add, however, this will not make the bounded models better approximations to the inviscid unbounded model. It is also immediately clear that  $R_1$ 's denominator has a zero for only one real value of  $h$ ;  $R_2$  has an infinite number of poles;  $R_3$ 's denominator has only two zeroes.<sup>4</sup> This is merely an extension of the remarks in sections 1 and 2.

#### 4. GENERAL DISCUSSION

In figures 2a, 2b, 2c, and 2d, the amplitudes of  $R_1$ ,  $R_2$ , and  $R_3$  are shown as functions of  $h$ . In figure 3 the phases of  $R_1$ ,  $R_2$ , and  $R_3$  are shown as functions of  $h$ . For  $R_2$  and  $R_3$ , the top is at 200 mb. The phases for negative  $h$ 's are not shown since the phases of  $R_1$ ,  $R_2$ , and  $R_3$  all equal  $0^\circ$  for negative  $h$ . Figures 4a and 4b merely reproduce figures 2a and 2c except that the top for  $R_2$  and  $R_3$  is taken at 10 mb. Similarly, figure 5 corresponds to figure 3—but with the new top height.

Concerning figures 2a, 2b, 2c, 2d, and 3, we may note the following:

1.  $|R_2|$  and  $|R_3|$  are approximately 40 percent smaller than  $|R_1|$  for  $h \gtrsim -20$  km.
2.  $|R_1|$ ,  $|R_2|$ , and  $|R_3|$  are in modest agreement for  $-20 \gtrsim h \gtrsim -0.1$  km.
3.  $|R_1|$  and  $|R_2|$  are in agreement for  $0 \gtrsim h \gtrsim -0.1$  km.
4.  $|R_3|$  is much smaller than  $|R_1|$  for  $0 \gtrsim h \gtrsim -0.1$  km.
5.  $|R_2|$  and  $|R_3|$  are smaller than  $|R_1|$  for  $h \gtrsim 10$  km.
6.  $|R_1|$ ,  $|R_2|$ , and  $|R_3|$  are in modest agreement for  $+5 \text{ km.} > h > +1.5 \text{ km.}$
7.  $|R_2|$  and  $|R_3|$  exhibit their first free oscillations for  $h$  between 6.5 and 7.0 km. while  $|R_1|$  exhibits its only free oscillation for  $h \approx 10.6$  km.
8.  $|R_3|$  exhibits an additional spurious free oscillation for  $h \approx 0.18$  km.
9.  $|R_2|$  exhibits spurious free oscillations for  $h \approx 0.5, 0.15, 0.062, \dots$  km., etc.
10. Because of 8 and 9 above, there is no meaningful agreement among  $R_1$ ,  $R_2$ , and  $R_3$  for  $0 < h \lesssim +1.5$  km.

When the top in the bounded models is raised to 10 mb., the following changes may be noted in figures 4a, 4b, and 5:

1. There is now good agreement among  $R_1$ ,  $R_2$ , and  $R_3$  for  $h < -1.5$  km.
2. There is excellent agreement between  $R_1$  and  $R_2$  at all negative  $h$ 's.
3. For  $0 > h > -1$  km.,  $R_3$  is too small.
4. For  $h > +5$  km. there is now modest agreement among all models. In particular, the first free oscillation in the bounded models occurs at  $h \approx 10$  km., which is quite near the correct value.
5. For  $0 < h < 5$  km. there is no longer any useful agreement between the bounded and unbounded models. In

<sup>3</sup> Equation (27) is a finite difference approximation to equation (26). Such approximations are by no means unique, and other differencing schemes would lead to quantitative though not qualitative differences in results. Quantitative differences are indicative of errors intrinsic to the use of finite differences.

<sup>4</sup> If, as is commonly done, we had taken  $\omega_2=0$  instead of (12) as our lower boundary condition (vis the baroclinic stability analysis in Thompson [6]), then we would obtain an expression for  $\omega_1$  with only one zero in its denominator. This value of  $h$  would be close to the smaller, spurious zero in the denominator of (32). When  $\omega_2=0$ , there is, however, another solution in two layer models for which  $\omega_1=\omega_2=\omega_0=0$ . This solution corresponds more closely to the free oscillation of the "real" atmosphere.

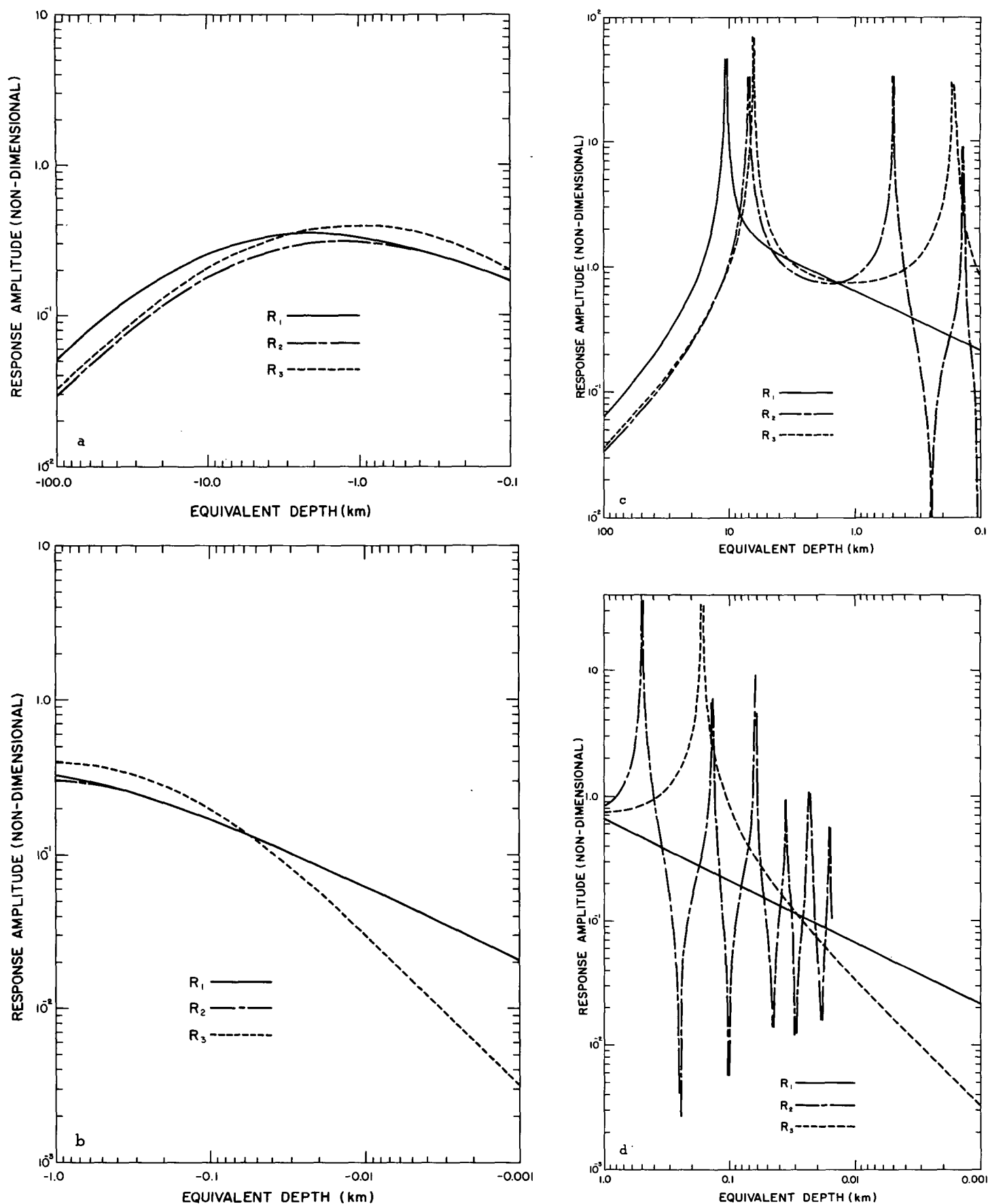


FIGURE 2.—(a) The amplitudes of the response functions for unbounded ( $R_1$ ), bounded continuous ( $R_2$ ), and bounded two layer ( $R_3$ ) atmospheres as functions of  $h$  for  $-0.1 \text{ km.} > h > -100 \text{ km.}$  The tops for the bounded models are at 200 mb. (b) Same as (a) but for  $-0.001 \text{ km.} > h > -0.1 \text{ km.}$  (c) Same as (a) but for  $100 \text{ km.} > h > 0.1 \text{ km.}$  (d) Same as (a) but for  $1 \text{ km.} > h > 0.001 \text{ km.}$

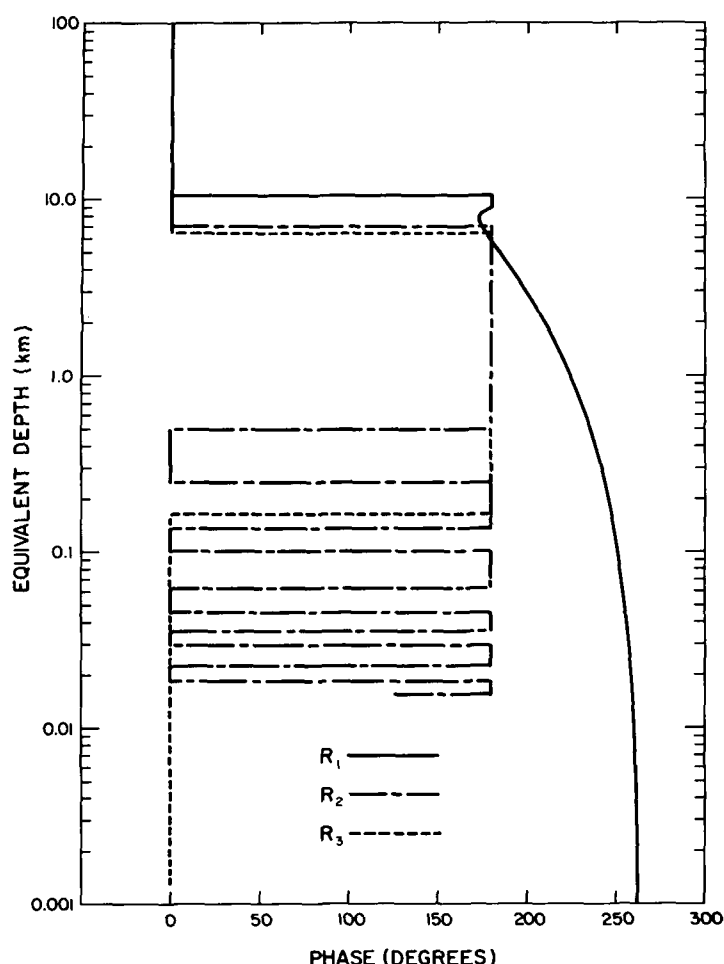


FIGURE 3.—The phases of  $R_1$ ,  $R_2$ , and  $R_3$  as functions of  $h$  for 100 km.  $> h > 0.001$  km. The tops for the bounded models are at 200 mb.

particular,  $R_3$  exhibits a spurious free oscillation for  $h \approx 0.79$  km., while  $R_2$  exhibits spurious free oscillations for  $h \approx 2.65, 0.98, 0.37, \dots$  km., etc.

The reasons for the spurious free oscillations in the bounded models have already been discussed and will not be dwelt on further. For large  $|h|$  the oscillatory fields' energy decreases with height approximately as  $\bar{\rho}$ . Clearly for models with tops, the upper boundary condition may violate this behavior severely if the top is too low. This is the case for a top at 200 mb.; it is not for a top at 10 mb. However, for  $h$  small and negative (corresponding to decay in the vertical with short vertical scale) the continuous bounded model becomes increasingly accurate; the two layer model underestimates the response because it cannot resolve short vertical scales. The lower the top, the better the resolution of a two layer model is. Hence, the two layer model with a 200-mb. top has better accuracy at small negative  $h$ 's than the one with a 10-mb. top. For small positive  $h$ 's (corresponding to oscillations which propagate vertically) both  $R_2$  and  $R_3$  are not even remote approximations to  $R_1$ . This is, moreover, not changed (except perhaps to make matters worse) by moving the top of the bounded atmospheres higher. This is seen in (23) where taking  $x_i \rightarrow \infty$  for small positive  $h$  does not lead to a defined limit. In the two layer model, poor resolution also

contributes to the problem, but it should be noted that higher resolution would not do more than produce a better approximation to the continuous bounded atmosphere.<sup>5</sup>

## 5. SPECIFIC CONCLUSIONS

The preceding discussion was phrased in general terms. We will now discuss some specific implications for numerical models.

### ROSSBY-HAURWITZ WAVES

Rossby-Haurwitz waves are free oscillations of the atmosphere for which the earth's rotation is of essential importance. At middle latitudes in the earth's atmosphere their phase speed in the absence of zonal flow is given approximately by

$$c \approx \frac{-\frac{1}{\sqrt{2}} \frac{\Omega a}{s^2}}{1 + \frac{1}{s^2} \left( \frac{\Omega^2 a^2}{gh} + 2n^2 \right)}, \quad (33)$$

where  $n$  is some latitude wave number (see Lindzen [3] for example). The  $h$  in (33) is that for which the atmosphere executes free oscillations. As we have seen in section 4,  $h \approx 10.6$  km. for an unbounded atmosphere. For bounded atmospheres there is more than one  $h$  for free oscillations, and only the largest one corresponds to free oscillations of a "real" atmosphere. For models with tops at 200 mb. even this  $h$  is quantitatively in error. As we see in figure 2c,  $h \approx 6.5$  km. in this case. From (33) we see that for  $n=2$  and  $s=5$  there will be an 8 percent error in  $c$  due to this particular error in  $h$ . Although seemingly small, this error alone will produce a  $90^\circ$  error in the phase of a planetary wave within about 5 days. This error can be reduced by moving the atmosphere's top higher. There remain, however, the possibly larger errors due to the spurious free oscillations. In connection with these, it must be noted that each free oscillation is associated with a particular vertical structure. In figure 6 we show the vertical structures of  $\omega$  for the two free  $h$ 's in the two layer model with a top at 200 mb. From figure 6 we may surmise that the effect of the spurious oscillations will be most noticeable at the middle level.

*A priori* it appears that the above described errors should be present in current numerical experiments. Thus far, however, no results of numerical experiments have been analyzed for this important possibility. In order for spurious waves to appear, they must in some way be activated. Errors in initial conditions may be adequate for this purpose. That the spurious waves may be baroclinically unstable (in numerical models) is another possibility. The question of whether or not the "real" Rossby-Haurwitz wave is the only one which may become baroclinically unstable is an open one—the answer to which is of obvious importance. Even in the absence of other sources the spurious oscillations will receive energy via

<sup>5</sup> It is possible in a multi-level to have a top at  $p=0$ . However, as a result of inevitable finite-difference errors, this is equivalent to having the top at some small, finite  $p$ .

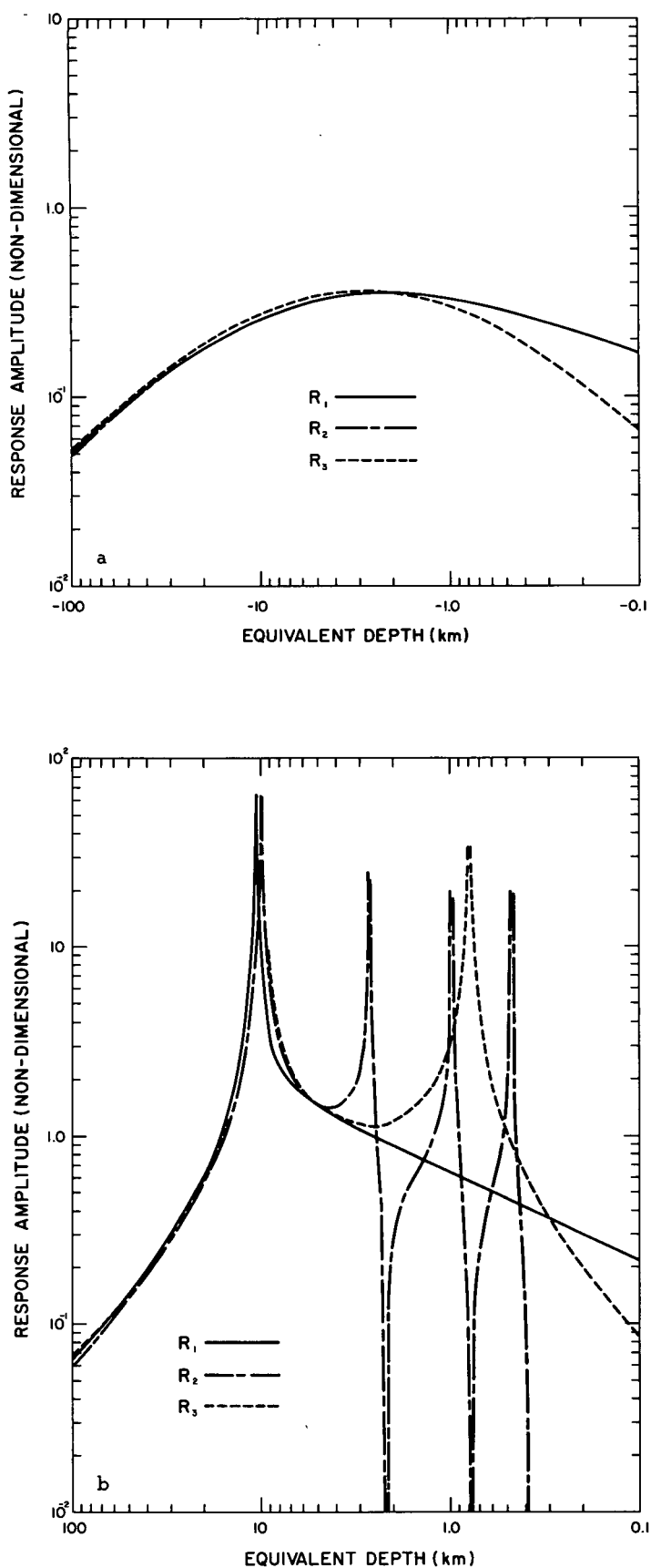


FIGURE 4.—(a) Same as figure 2a but the tops for the bounded models are at 10 mb. (b) Same as figure 2c but the tops of the bounded models are at 10 mb.

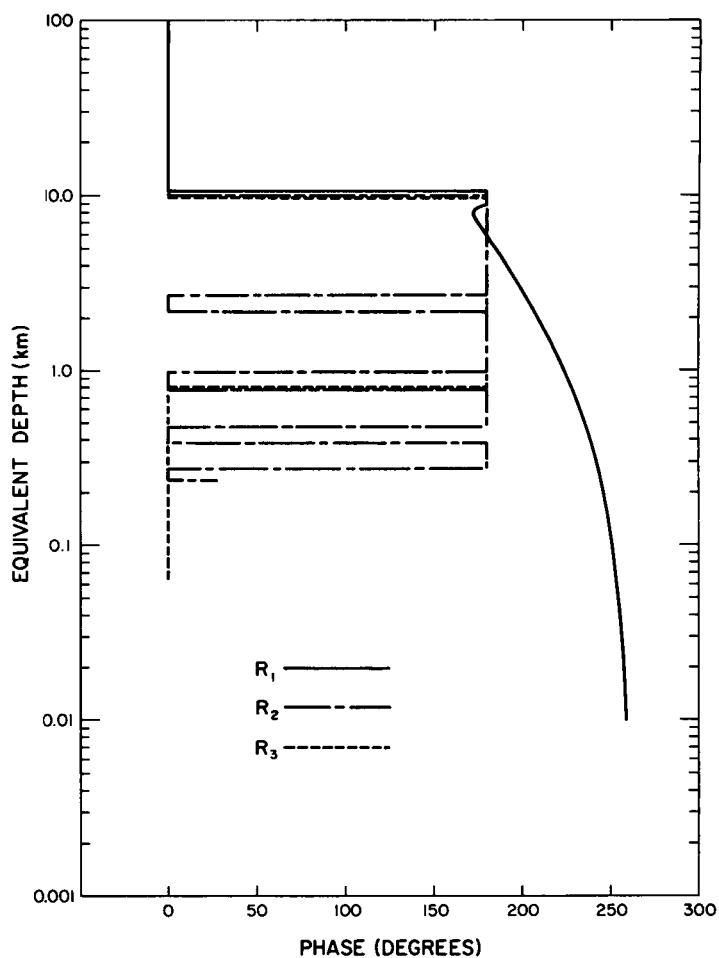


FIGURE 5.—Same as figure 3, but the tops for the bounded models are at 10 mb.

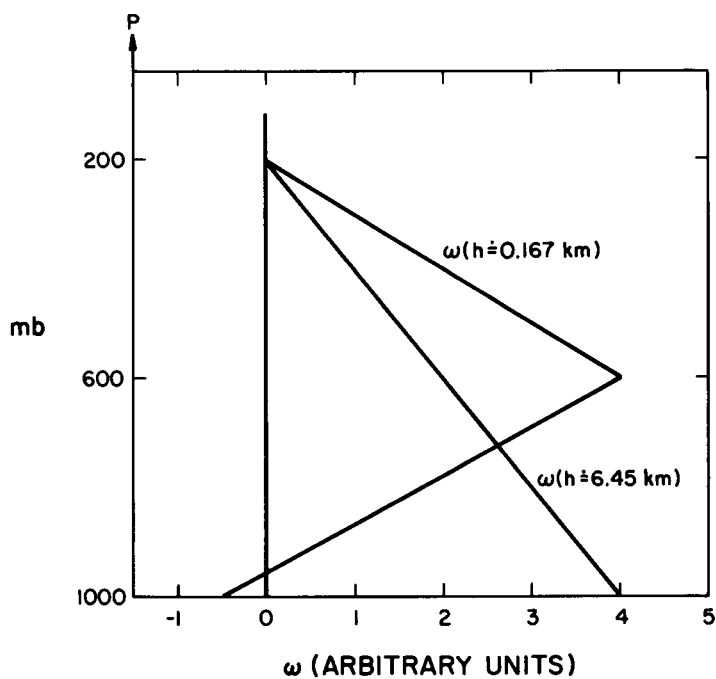


FIGURE 6.—The vertical structures of the two free modes occurring in the two layer model with a top at 200 mb. The mode corresponding to an equivalent depth of 0.167 km. is spurious.

TABLE 1.—Response amplitude  $|R|$  and phase angles  $\varphi$  for diurnal and semidiurnal oscillations in model atmospheres summarized from figures 2–5

$h$	Migrating solar ( $\sigma=2\Omega$ , $s=2$ ) semi-diurnal		Migrating solar ( $\sigma=\Omega$ , $s=1$ ) diurnal			
	7.85 km. $ R $ $\varphi$	2.11 km. $ R $ $\varphi$	–12.25 km. $ R $ $\varphi$	–1.75 km. $ R $ $\varphi$	+0.699 km. $ R $ $\varphi$	+0.122 km. $ R $ $\varphi$
Model 1	2.29    172.5°	0.919    208.4°	0.234    180°	0.349    180°	0.549    230.2°	0.234    248.9°
Model 2a—( $R_2$ —top at 200 mb.)	3.82    0.0°	0.768    180°	0.160    180°	0.308    180°	1.23    180°	0.326    0.0°
Model 3a—( $R_3$ —top at 200 mb.)	2.49    0.0°	0.856    180°	0.181    180°	0.382    180°	0.779    180°	1.56    0.0°
Model 2b—( $R_2$ —top at 10 mb.)	3.02    180°	0.146    180°	0.233    180°	0.348    180°	0.226    180°	0.482    0.0°
Model 3b—( $R_3$ —top at 10 mb.)	3.24    180°	1.22    180°	0.250    180°	0.345    180°	4.56    0.0°	0.109    0.0°

nonlinear exchanges. Once excited, there is no reason at present to suppose that spurious oscillations will be preferentially damped in numerical experiments since, as shown by Lindzen [3], small values of  $h$  may be associated with large horizontal scales. Small values of  $h$  are associated with small vertical wavelengths, but even  $h$ 's of the order of  $10^{-1}$  km. are associated with vertical wavelengths of the order of 10 km., and excessive damping of such large wavelengths could result in poor modeling on other grounds.

#### THERMAL TIDES

Thermal tides are forced oscillations as described in section 2. They are excited primarily by the daily variations in insolation absorption by ozone and water vapor. For each tidal component we specify  $\sigma$  and  $s$ , and solve (4) for an infinite set of  $\Theta_n$ 's and the accompanying  $h_n$ 's. The excitation for the particular component is expanded as in (13), and (7) is solved for each  $n$ . The most important tidal components are the migrating solar semidiurnal ( $\sigma=2\Omega$ ,  $s=2$ ) and the migrating solar diurnal ( $\sigma=\Omega$ ,  $s=1$ ). For the former, the most important solutions of (4) (Hough Functions) are associated with equivalent depths ( $h_n$ 's) of 7.85 km. and 2.11 km. For the latter the most important Hough Functions are associated with equivalent depths of –12.25 km., –1.75 km., 0.699 km., and 0.122 km. To the extent that tides are excited by absorption by water vapor, figures 2–5 show the effect of different models on the surface pressure response. The results are summarized in table 1. This table is self explanatory, and the differences among the models are evident. Particularly noteworthy is the phase error for the main semidiurnal mode in the bounded model when the top is at 200 mb.

It is important at this point to note some differences between the two layer model used here and those used in actual numerical experiments. For example, we have here assumed that (4) is solved "exactly" in order to obtain

the  $h_n$ 's. In numerical experiments it is, in effect, solved by finite differences. Moreover, effects of mean flow, ignored here, are automatically included in numerical experiments. As a result of these differences, the  $h_n$ 's applicable to numerical experiments may differ from those shown in table 1. In particular, if the appropriate  $h$  for the main solar semidiurnal mode is slightly smaller than 7.85 km., then we see from figure 2c that the response of atmospheres with tops at 200 mb. will be much greater than shown in table 1. Finally, we note that dissipation, neglected here, exists in both the real and the numerical atmospheres. The effect of boundary layer dissipation on the response phase has been mentioned in section 3. A measure of the importance of dissipation in the real atmosphere is given by the fact that the predicted peak in the semidiurnal surface pressure oscillation is near 0900 hr. (neglecting dissipation) while the observed peak occurs between 0930 and 1000 (i.e., dissipation appears to move the peak closer to local noon). For models with tops at 200 mb., the predicted peak occurs at 1500 hr. It should be observed to occur between 1200 and 1500 hr. in numerical models depending on how dissipation is modelled.

#### REFERENCES

1. L. A. Dikii, "The Terrestrial Atmosphere as an Oscillating System," *Izvestiya, Atmospheric and Oceanic Physics*, English Edition, vol. 1, No. 5, May 1965, pp. 275–286.
2. T. W. Flattery, "Hough Functions," *Technical Report No. 21*, Department of the Geophysical Sciences, University of Chicago, Mar. 1967, 175 pp.
3. R. S. Lindzen, "Planetary Waves on Beta-Planes," *Monthly Weather Review*, vol. 95, No. 7, June 1967, pp. 441–451.
4. D. Nunn, "A Theoretical Study of Tides in the Viscous Region," M.S. Thesis, McGill University, Montreal, May 1967.
5. M. Siebert, "Atmospheric Tides," *Advances in Geophysics*, vol. 7, Academic Press, New York, 1961, pp. 105–182.
6. P. D. Thompson, *Numerical Weather Analysis and Prediction*, Macmillan Co., New York, 1961, 170 pp.

[Received August 17, 1967; revised September 25, 1967]